CL 02-0299 FINAL

Field Emission Cathodes for Electrodynamic Tethers: Identifying Compatible Cathode Materials

Colleen Marrese-Reading[1], Bill Mackie[2], Chris Dandeneau[2], Michael Quinlan[3], Bruce Koel[3], Jay Polk[1]

1 Jet Propulsion Laboratory, California Institute of Technology, Pasadena, CA 91109
(818) 354-8719, colleen.m.marrese@jpl.nasa.gov
(818) 354-9275, james.e.polk@jpl.nasa.gov
2 Applied Physics Technologies Inc., McMinnville, OR
(503) 434-5550, bmackie@a-p-tech.com
cdandeneau@a-p-tech.com
3 University of Southern California, Los Angeles CA 90089-1062
(213)740-4126, koel@chem1.usc.edu
(213) 740-6282, mquinlan@chem1.usc.edu

Abstract.
Several material combinations were considered as candidates for the electrodynamic tether application in the investigation discussed in this paper. Critical characteristics like work function, resistance, sputter yield and sensitivity to oxidizing environments were considered. The material investigation included, ZrC/Mo, Mo, MgPt, Pt, NbC/Nb, NbNi/Nb, Nb, RuTa/Ta, Ru/Ta and Ta. The results of the measurements suggest that NbC/Nb, NbNi/Nb, and MgPt are the most promising candidates.

INTRODUCTION

Field emission cathodes are under development for electrodynamic tether systems for orbit control in low Earth orbit environments which are primarily atomic oxygen. These systems require 100 –10000 mA from the electron source. The space charge in this environment will limit the cathode current density to ~10 mA/cm^2 if electrons are emitted with 30 eV energies [Marrese et al., 2000] at a 300 km altitude. These cathodes are primarily operated in UHV environments at 10^{-9} Torr. In much higher pressure environments, the tips can get contaminated to change the work function and tip conductivity and get sputtered to change the tip radius of curvature [Brodie et al.,1994, Chalamala et al., 1998., Marrese et al., 2001]. These environmental effects can significantly degrade cathode performance because they are exponentially sensitive to changes in both work function and tip radius. The cathode current is also sensitive to changes in the emitting tip surface conductivity from contamination[Shaw,2000].

Many experimental results have shown an exponential degradation in current with exposure to oxygen [Brodie et al.,1994, Chalamala et al., 1998, Marrese et al., 2001] from both temporary and permanent damage to the tips. Temporary degradation in cathode performance will occur quickly while operating in oxygen-rich environments from both physical and chemical adsorption of oxygen. Absorption of oxygen can also cause permanent performance degradation for sufficiently long exposures. [Marrese et al., 2001] Tip sputtering by self-generated ions can cause permanent damage to the tip radii and cathode performance if the cathode operating voltages are high enough to generate ions between the tips and gates which strike the tips with energies which exceed the energy threshold for sputtering the tip material. It has been argued that performance degradation in contaminating environments is also attributable to changes in work function from ion implantation.

The objective of this cathode development program is to identify the cathode materials required for the electrodynamic tether application. Fabricating Spindt-type field emission cathodes with many different tip materials to directly evaluate their performance in oxygen environments is prohibitively expensive for this program. Therefore, the stability of the critical properties of many potential cathode materials in oxygen environments is being investigated to identify the best field emission array cathode material candidates for the electrodynamic tether application. The required cathode material characteristics include low work functions to provide ≥10 mA/cm^2 at extraction voltages which are below the limit for the formation of ions with energies which exceed the energy threshold for sputtering the cone material. These materials must be stable while operating in oxygen-rich environments.

The strategy and results of this investigation are discussed in this article. The material selection process is described with the required material characteristics. The sensitivity of the cathode material characteristics to the oxygen environment will be presented in the form of work function and conductivity measurements taken before and after the oxygen exposures and in the thickness of the surface oxide formed.

CATHODE MATERIALS

Desired Characteristics

It has been shown that conventional Spindt-type cathode materials are not compatible with oxygen environments; therefore, suitable materials must be identified which also have the material characteristics required for field emitter cathodes. These properties include a low and stable work function and good conductivity in oxygen-rich environments. The tolerable work function depends on the gate aperture diameter, tip emission uniformity (Δs), tip packing density, and operating voltage limitations. A cathode in equilibrium with its environment should maintain a work function no higher than 4.8 eV if gate voltages as high as 90 V are tolerable. If lower operating voltages are necessary, lower work function materials will be required. For example, experimental results suggest that the operating voltage limitation is between 60 and 70 V for ZrC-coated Mo cathodes operating in oxygen environments. If the equilibrium work function of ZrC in oxygen environments is 4.4 eV (change in work function estimated from exposure experiments after 8.9×10^{-6} Torr-hours), then required operating voltages will be between 40 and 80 V depending on the emission uniformity quantified by Δs and the cathode feature sizes. However, after this exposure, the performance of the cathode continued to decay due to further changes in work function and/or surface conductivity. An attempt to compensate for the current decay by increasing the gate voltage actually lead to accelerated decay rates. This result may be due to tip sputtering and/or charging in the surface films during the exposures with the cathodes operating. Maintaining sufficient conductivity in an oxygen-rich environment and operating below the voltage threshold for sputtering are both critical in successfully integrating field emission cathodes with space-based applications.

The Δs parameter for a cathode also significantly affects the cathode performance, but with a linear relationship. Variation in tip radius of curvature across the array is captured in the Δs parameter. A smaller Δs value is representative of a more uniformly emitting array of cones. The current cathode configuration has gate aperture radii of 4500 Å. Δs values estimated from experiments performed on ZrC/Mo cathodes in this program were between 32 and 0.9 at <100 V (although values as low as 0.1 have been demonstrated at SRI International with Mo cathodes at much higher operating voltages, >100 V). With demonstrated Δs values, lower work function materials with the aforementioned characteristics will be required to achieve 10 mA/cm^2 at the desired operating voltages of 30 V. Cathodes with smaller gate aperture diameters will demonstrate lower Δs values at such low voltages to further improve cathode performance.

Changes in surface film conductivity will also affect the tolerable work function limit and negatively affect the cathode performance. Some materials oxidize quickly in an atomic oxygen environment with a thickness limited only by the thickness of the base material as believed to be the case with Mo. An oxide film on the tips can increase or decrease the work function significantly. An oxygen film on the surface typically increases the work function. Perhaps most importantly, as noted above, an oxide film will reduce the surface conductivity which results in charging up of the film leading to further current degradation [Shaw, 2000]. Both responses to the oxygen environment will negatively affect the performance of the cathode by decreasing its stability and increasing its operating voltages to regimes that could significantly decrease the cathode lifetime. Therefore, some materials which will form conductive oxides in oxygen-rich environments have been identified as cathode material candidates. The required conductivity for the surface films is uncertain, but most likely depends on the film thickness.

Table 1. Cathode current densities for various operating voltages, V_g, work functions, ϕ, packing densities, pd, tip radii, r_t, spread in tip radii, Δs, gate aperture radii, r_g, tip half cone angle, β_c.

pd (tips/cm^2)	β_c	r_t	Δs	r_g	ϕ	V_g	J (mA/cm^2)
10^7	0.26	40	2	4500	3.8	35	0.2
10^7	0.26	40	2	4500	3.8	40	2.6
10^7	0.26	40	2	4500	3.8	50	89
10^7	0.26	40	2	4500	4.1	50	15.4
10^7	0.26	40	100	4500	4.1	60	4.6
10^7	0.26	40	100	4500	4.1	70	30.0
10^7	0.26	40	500	4500	4.1	70	7.6
10^7	0.26	40	2	2000	3.8	35	9.3
10^7	0.26	40	2	2000	4.1	40	12.5
10^7	0.26	40	10	2000	4.1	40	2.5
10^7	0.26	40	10	2000	4.1	50	68.0
10^7	0.26	40	100	2000	4.1	40	0.2
10^7	0.26	40	100	2000	4.1	50	6.8
10^7	0.26	40	500	2000	4.1	60	14.0
10^7	0.26	50	500	2000	4.1	40	0.006
10^7	0.26	40	2	4500	3.8	60	1.08
10^7	0.26	40	2	4500	4.4	60	49.0
10^7	0.26	40	2	4500	4.6	60	17.0
10^7	0.26	40	2	4500	4.7	60	10.4

Materials Under Investigation

Several materials have been identified in this investigation as promising candidates for the tether application. They have been chosen because of their excellent work functions and anticipated superior resistance to oxidation and/or the anticipated formation of conductive oxides in oxygen-rich environments. These materials include Mg on Pt (Pt/Mg), NbC on Nb (Nb/NbC), NbNi on Nb (Nb/NbNi), C on Pt (Pt/C), MgPt on Pt (Pt/MgPt), and Ru on Ta (Ta/Ru). Mo and ZrC on Mo (Mo/ZrC) are also being included in the investigation for comparison. Pt/Mg was selected because it forms a conductive oxide with an excellent work function. Thin MgO surface films on field emission cathodes have demonstrated acceptable conductivity. The work function of MgO has been measured to be 3.1-4.4 eV [Tsarev, 1955], and the measured work function of Pt is 5.32 eV [Femenko, 1966], however, the work function of MgO on Pt has been measured to be 3.19 [Jentzsch, 1908] and 3.31 eV [Spanner, 1924]. Since intermetallic films can be more stable in oxidizing environments Pt/Mg and Pt/MgPt film combinations are both under investigation. There are concerns about observed electron-induced oxygen desorption from the MgO on the cathode surface affecting the cathode stability. This process could expose Mg which could be easily sputter removed and cause increases in cathode work function and tip radii. The oxygen environment could sufficiently replenish the desorbed oxygen before this process occurs. Nb/NbC was selected because of its excellent work function, a developed Spindt-type field emission cathode fabrication process, and some promising results recently released [Mackie, et al., 2001]. NbC cones have been deposited into 0.4 um diameter gate apertures with excellent results. The cathode performance was not affected by operating in ~$5x10^{-7}$ Torr of oxygen for 40 min. Nb/NbNi was selected because of fabrication experience, anticipated stability in oxidizing environments, decent work function, and good NiO conductivity. It is anticipated that the intermetallic films will offer a higher resistance to oxidation than the film constituents. Ru and Ta film combinations were selected because of the work function and conductivities of the materials and their oxides. Silicon FEA cathode tips with Ta and then Ru films deposited on them were oxidized with excellent results. [Yoon et al., 2000] The RuO_2 surface oxide was conductive and the work function was identical to the work function of Ta, 4.1 eV. The RuO_2-Ta interface was incredibly stable, prohibiting oxidation of the Ta base film.

MATERIALS CHARACTERIZATION

Material characterization was performed both theoretically and experimentally, to compare several characteristics of the various materials considered in our investigation.

Theoretical

Penetration Depth

SRIM (Stopping and Range of Ions into Matter)[1] [Ziegler et al. 1985] was used to approximate the ion penetration depth in various cathode candidate materials. SRIM consists of a group of programs which are used to determine the stopping range of ions into matter using a full quantum mechanical treatment of collisions between ions

impinging on a target and the atoms in that target. Chemical reactions with the target are not considered. The results of the calculations with SRIM are presented in Table 2.

Sputter yield

TRIM (Transport of Ions in Matter) was used to estimate and compare the sputter yields of various cathode candidate materials. TRIM can be used to determine the final 3-D distribution of the ions and also all kinetic phenomena associated with the ion's energy loss: target damage, sputtering, ionization, and phonon production. It is not capable of considering the effects of chemical reactions between the ions and target material on the sputter yield. 500 ions were bombarded the targets to obtain the statistics for the sputter yield estimates. The results of the calculations with SRIM are presented in Table 2. The calculated sputter yields are compared for many of the cathode candidate materials.

Table 2. Material penetration depth, d, and sputter yield, Y, for atomic oxygen ions with the energies identified and targets with the materials and densities identified.

Material (t(nm))	Density (g/cm^3)	d (nm) 50 eV	d (nm) 100 eV	d (nm) 200 eV	Y (atoms/ion) 100 eV
Ir	2.24	0.3	0.4	0.5	0.020
Mg	1.73	0.9	1.3	1.9	0.584
Mo	10.20	0.4	0.5	0.7	0.136
Nb (10)	8.57	0.4	0.6	0.8	0.120
NbC (10)	7.60		0.7		0.050 (Nb) 0.044 (C)
Pt	2.14	0.3	0.4	0.6	0.022
PtC					
Ru (10)	1.23	0.3	0.4	0.6	0.148
RuTa					
Ta	1.66	0.4	0.5	0.7	0.014
Zr (10)	6.49	0.5	0.8	1.1	0.128
ZrC	6.73	0.5	0.6	0.8	0.054 (Zr) 0.038 (C)

Experimental

Sample Preparation-Film Deposition

The films under investigation were deposited at Aptech Inc. on 0.5 mm-thick silicon wafers. Si wafers were sputter cleaned by a 260 V Ar ion beam for 5 minutes before the films were deposited on the substrates. Ti films were deposited on the Si wafers before film deposition to improve adhesion. Ti film thickness was 10 nm. ZrC was evaporated from zone refined single crystal onto Mo for the ZrC/Mo sample. NbNi was evaporated from a NbNi alloy target onto the Nb film for the NbNi/Nb sample. Mg and Pt were co-deposited onto the Pt film for the MgPt/Pt sample. Ru and Ta were co-deposited onto the Ta film for the RuTa/Ta sample. A slightly higher concentration of Ru is expected in the surface film. The thickness of the films on the samples are given in Table 3.

Table 3. Film combinations identified for the samples prepared and the thicknesses of the various films deposited.

Sample Identity	Surface Film	thickness (nm)	Base film	thickness (nm)
MgPt	MgPt	200		
Mo			Mo	300
Nb			Nb	300
NbC/Nb	NbC	10	Nb	500
NbNi/Nb	NbNi	10	Nb	300
Pt			Pt	200
PtC/Pt	PtC	10	Pt	200
Ru/Ta	Ru	10	Ta	300
RuTa/Ta	RuTa	10	Ta	300
Ta			Ta	300
ZrC/Mo	ZrC	10	Mo	300

Sample Exposures to Atomic Oxygen

The material samples were exposed to ozone environments to simulate a dose of atomic oxygen to the cathodes similar to the dose that they will experience in a LEO environment. An UltraViolet Ozone Cleaning System (UVOCS) was used in these exposures. A new lamp in this system produces 60-100 ppm of ozone. It is estimated that this lamp has been used for <1000 hours. The lamp intensity typically decays by 10 % in 1000 hours. Therefore, the ozone PPM in the source should range between 50 and 100 at atmospheric pressure. Ozone easily dissociates into molecular and atomic oxygen upon impacting the material surface providing a thermal flux of atomic oxygen to the samples. The lowest PPM of ozone approximated for this system is 50. Assuming temperatures in the ozone source are approximately 300K, the flux of ozone to the samples is ~$4x10^{22}/m^2/s$. In LEO ambient at 300 km, the flux of atomic oxygen to the cathodes would be$1.1x10^{17}/m^2/s$. A 30-day exposure would result in a total dose of $2.8x10^{23}/m^2$. A 1-month exposure to the LEO environment could be accomplished with a 7-second exposure to ozone in the ozone source used. The samples were exposed to ozone for 5 and 20 minutes to determine if the films would passivate themselves after such long exposures, if the oxide films formed were stable, and how the extreme exposures would affect the cathode material properties.

AES-Argon Ion Sputter Depth Profiling

Surface oxide thickness on the films was characterized both before and after the films were exposed to atomic oxygen environments. The native oxide film thickness was determined in addition to the surface oxide thickness after exposure to ozone for 5 and 20 minutes. Depth profiling was conducted using a PHI 660 Scanning Auger Microprobe equipped with a single pass cylindrical mirror analyzer and PHI **04-303** differentially pumped sputter ion gun. Auger electron spectra were acquired at a chamber pressure of approximately 10^{-8} Torr with a 3 keV electron beam. The energy of the argon ions sputtering the films was 2 keV and current was 25 mA with a 2x2 mm raster. The ions bombarded the samples at 60° from the surface normal. The Auger spectra acquired represents, on average, the composition of the top 1 nm of the surface, but can detect electrons from as deep as 10 nm below the surface.

The films were sputtered at various time steps separated by Auger spectra measurements to produce plots of the variation in surface species in time, which can be converted to depth with the material sputtering rate. The sputtering rate of the thin film alloys was estimated employing the assumption that the surface film has been removed when the substrate signal reaches 50% of its final intensity. It is then assumed that the oxide film is removed with the same sputter rate to approximate the thickness of the surface oxide. The surface oxide thickness is approximated by the material sputter rate and time required for the oxygen signal intensity to drop to 50% of its original value. The results of the depth profiling are shown in the following several figures. Table 4 presents the calculated thickness of the surface oxides for the material combinations investigated.

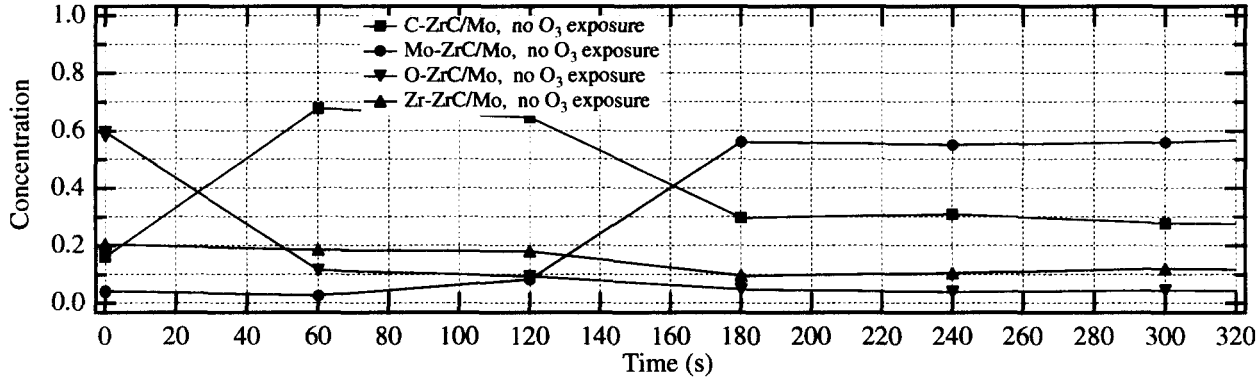

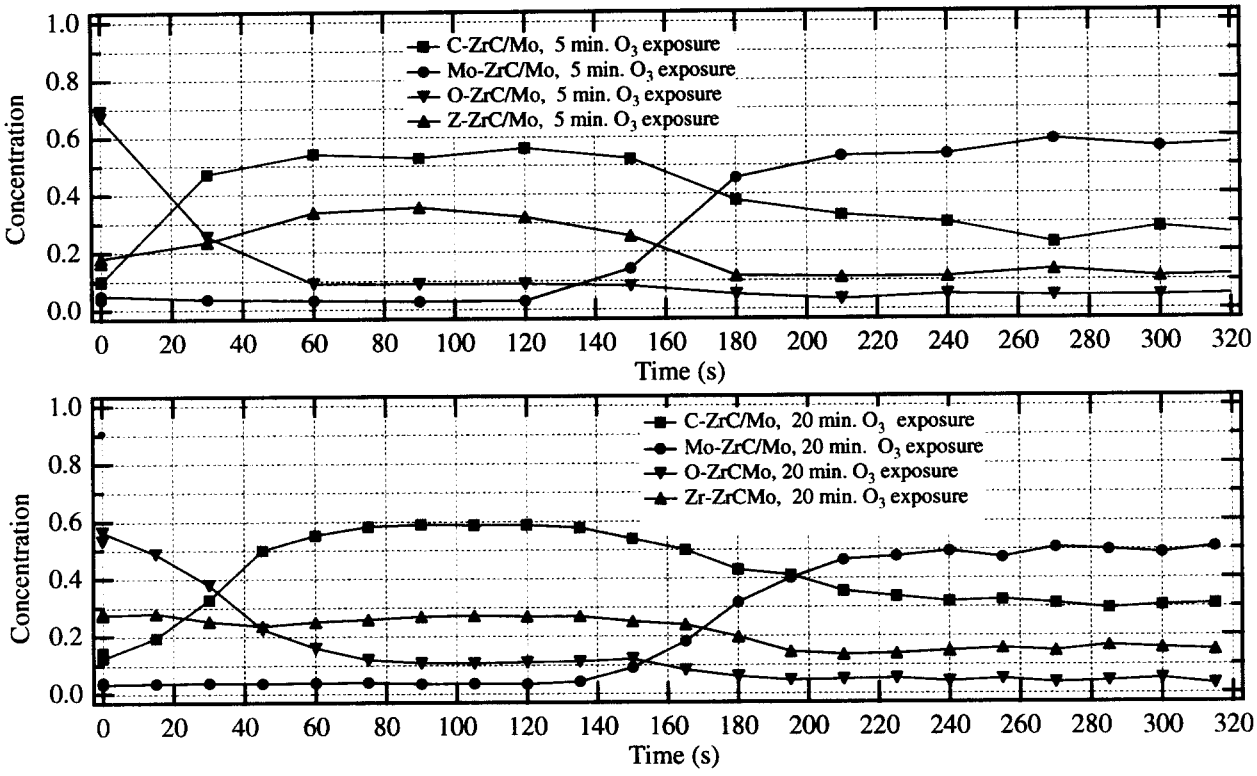

Figure 1. Surface component concentrations for the ZrC/Mo samples exposed to ozone for 0, 5, and 20 min.

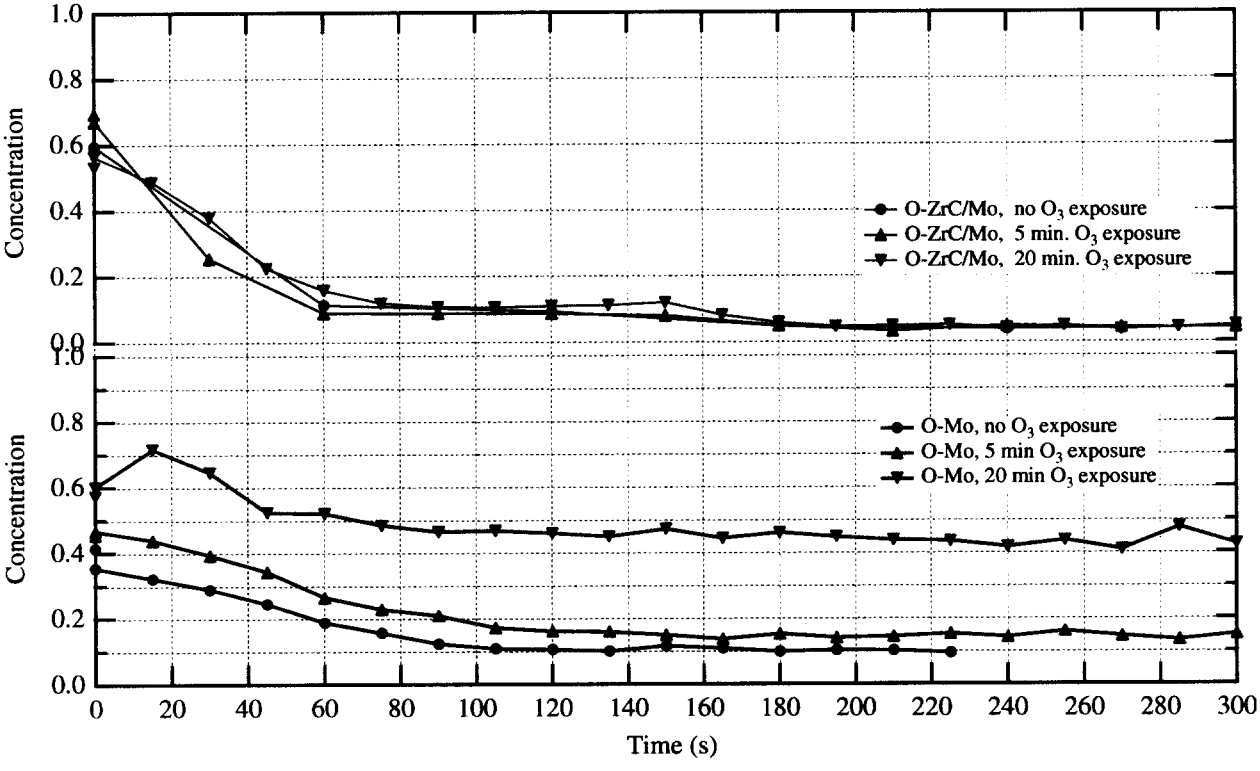

Figure 2. Oxygen concentrations for Mo and ZrC/Mo films.

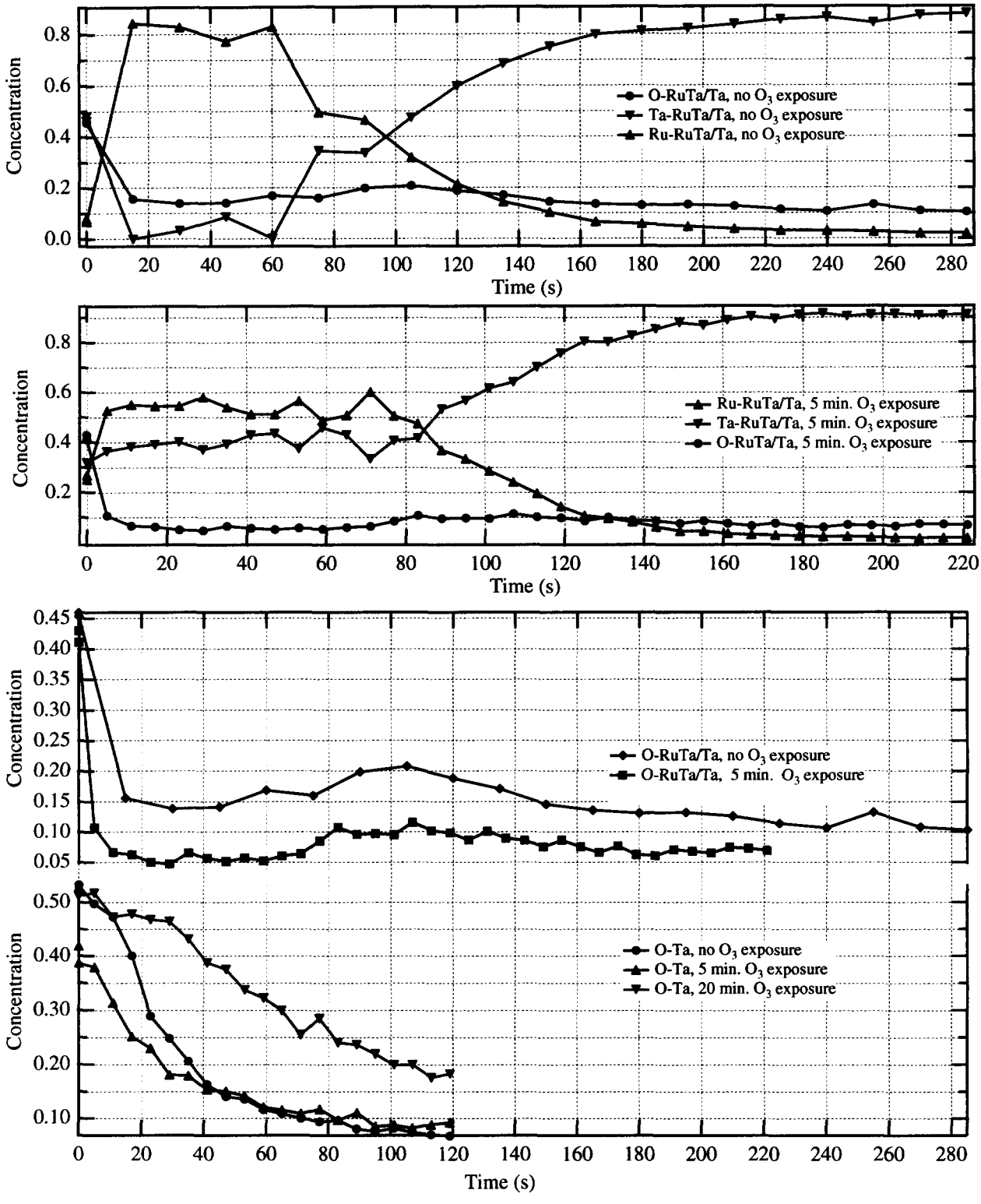

Figure 3. Surface component concentrations for Ta and RuTa/Ta films.

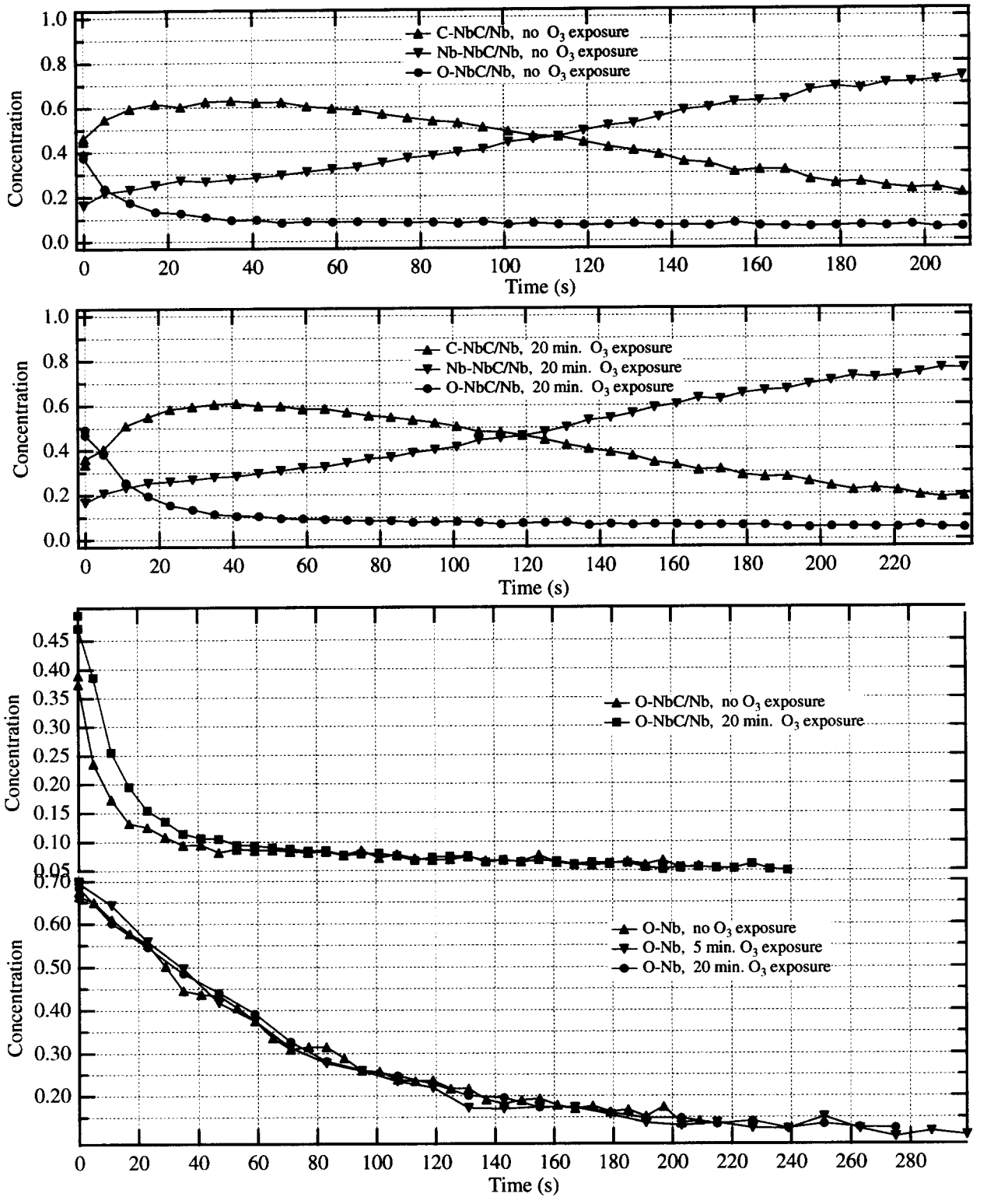

Figure 4. Oxygen concentrations for Nb and NbC/Nb films.

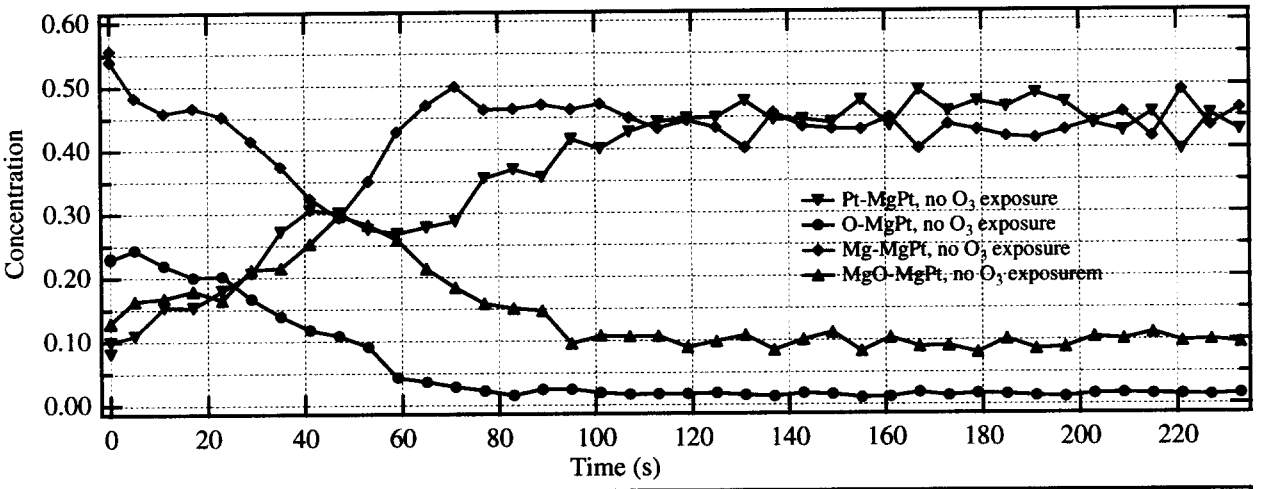
Concentration
Time (s)
Pt-MgPt, no O_3 exposure
O-MgPt, no O_3 exposure
Mg-MgPt, no O_3 exposure
MgO-MgPt, no O_3 exposure

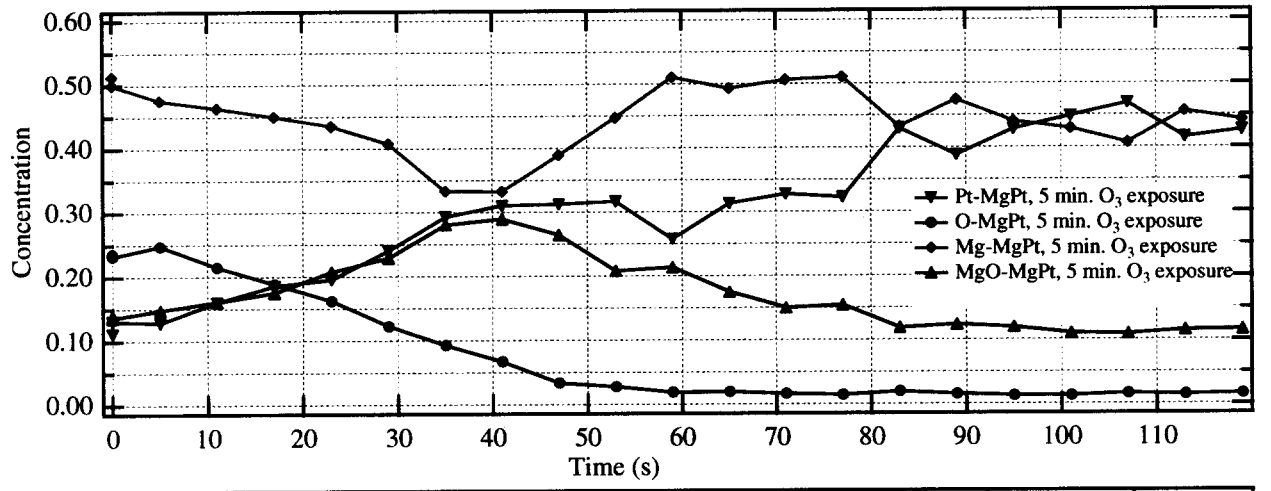
Concentration
Time (s)
Pt-MgPt, 5 min. O_3 exposure
O-MgPt, 5 min. O_3 exposure
Mg-MgPt, 5 min. O_3 exposure
MgO-MgPt, 5 min. O_3 exposure

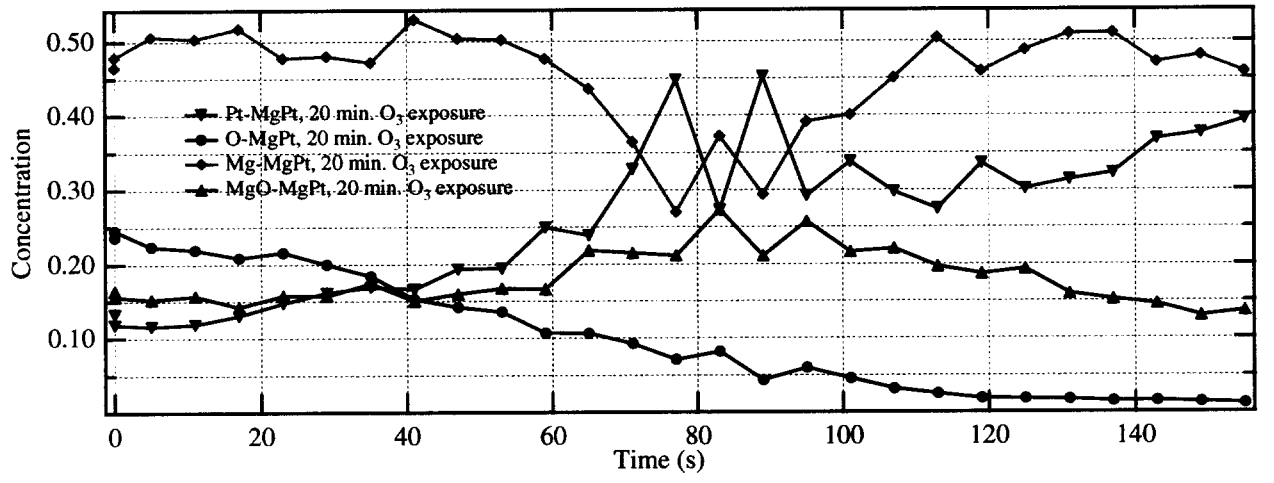
Concentration
Time (s)
Pt-MgPt, 20 min. O_3 exposure
O-MgPt, 20 min. O_3 exposure
Mg-MgPt, 20 min. O_3 exposure
MgO-MgPt, 20 min. O_3 exposure

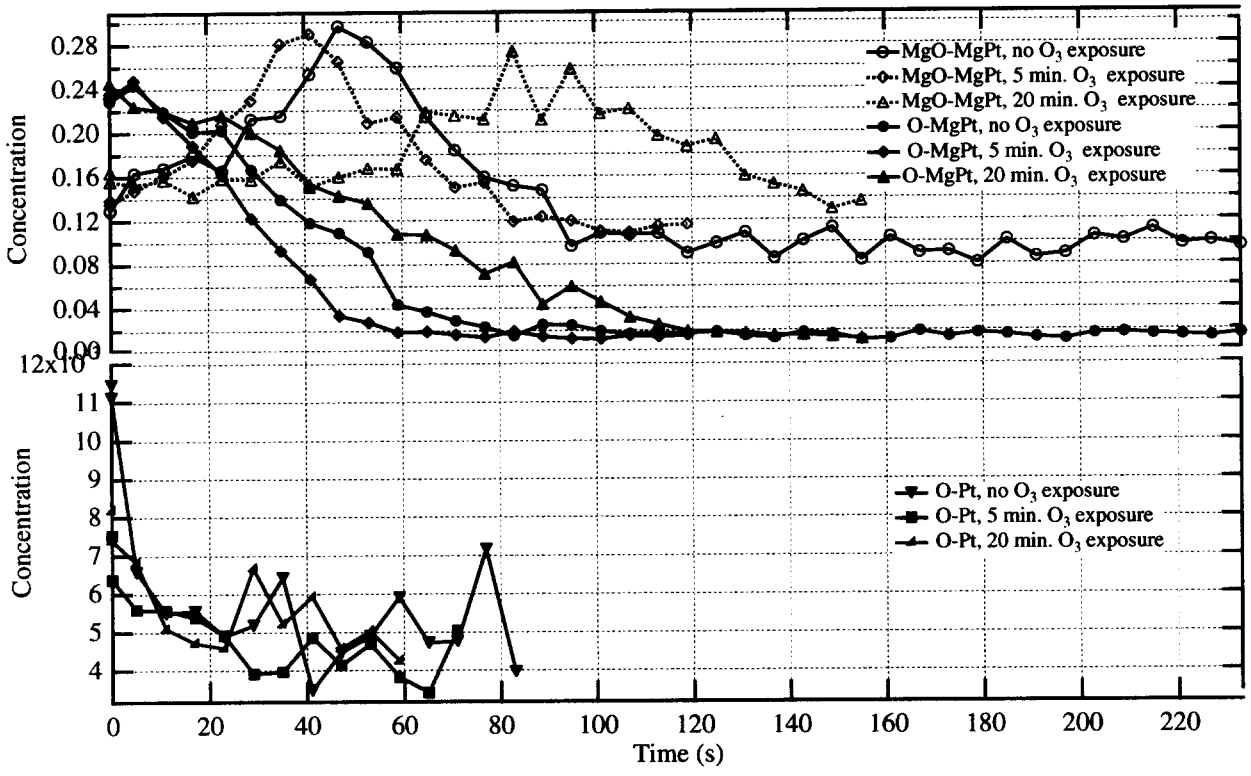

Figure 5. Surface concentrations for Pt and MgPt films

Table 4. Thickness of the surface oxide films estimated for samples not exposed to ozone and for the samples exposed to 5 and 20 min. of ozone.

Material	Native Oxide (nm)	5 min. O_3 Exposure (nm)	20 min. O_3 Exposure (nm)
Mg/Pt			
MgPt/Pt			
Mo			
Nb	5.39 (0.06 nm/s)	5.39	5.39
NbC/Nb	0.59 (0.06 nm/s)		0.84
NbNi/Nb			
Pt			
C/Pt			
Ru/Ta			
RuTa/Ta	0.63 (0.077 nm/s)	0.25 (0.085 nm/s)	
Ta			
ZrC/Mo	3.0	1.6	3.0
ZrPt/Pt			

Surface Film Resistivity Measurements

The surface resistance of some of the material samples were measured before and after they are exposed to atomic oxygen. The results of the measurements are presented in Table 5. Not all of the samples were exposed to the ozone environment for the post-exposure resistance measurements. These measurements were taken using a Veeco 4-pt probe.

Table 5. Resistance of the surface oxide films measured for samples not exposed to ozone and for the samples exposed to 5 and 20 min. of ozone.

Material	Resistance (mOhm)	
	Native Oxide	20 min. Exposure to O_3
MgPt	30	30
Mo	74	
Nb	74	
NbC/Nb	43	
NbNi/Nb	50	45
Pt	47	45
PtC/Pt	26	
Ru/Ta	54	
RuTa/Ta	114	127
Ta	261	265
ZrC/Mo	176	173

Work Function Measurements

The work function measurements were performed at Applied Physics Technologies (Aptech) Inc. using the photoelectron method. This method does not require exacting vacuum conditions and is straight forward in its application. A xenon light source and monochrometer are used to illuminate the planar surface to produce the desired photoelectrons. The NIST traceable source beam calibration is performed before and after the samples are changed. The induced current is measured by an electrically floating probe on the sample. The theoretical basis for this method was developed by Fowler in 1931.

The work functions of the selected materials were identified both before and after the samples were exposed to oxygen environments in approximately 10^{-8} Torr. The work function measurements are presented in Table 6. Auger electron spectra were also obtained at Aptech Inc. for many of the samples to identify surface composition and changes in the surface composition which influence the material work function.

MgPt Film #1

This particular film was loaded into the UHV chamber 34 days after its deposition. The first set of photoemission data was recorded 24 hours after a 5×10^{-8} Torr vacuum had been established. The work function appeared to be between around 4.1 eV. While the platinum level was around 3%, Auger scans showed no carbon content. Oxygen and magnesium comprised the rest of the film surface, with each element averaging about 48.5%. Another data set taken after 240 hours yielded a work function around 4.4 eV. The platinum level dropped to 1%, while carbon content was around 4%. Magnesium and oxygen levels showed little change. The UHV chamber was baked for 11 hours at 150°C. The work function after this baking was found to be about 4.3 eV. Auger scans showed that while magnesium and carbon levels declined by 5%, carbon content rose from 4% to about 14.5%. No significant changes were noticed in the platinum level.

Nb Film #1, Nb Film #2

Both of these niobium films were loaded into the UHV system 4 days after they were deposited. The comparable data gathered from each film is the reason why they are discussed together. The first set of photoemission figures was taken around 2 hours after a 5×10^{-8} Torr vacuum was achieved. Work functions for both films were about 4.25 eV – 4.3 eV. The work function of Nb Film #3 appeared to be slightly lower. Not surprisingly, auger scans showed Nb Film #3 with a higher carbon level (20% versus 15%) and a lower oxygen percentage (57% versus 63%) when compared to Nb Film #2.

Subsequent data was taken around 25 and 44 hours after a suitable vacuum was achieved. Nb Film #2 had a work function of 4.6 eV at 25 hours and 4.7 eV after 44 hours. For Nb Film #3, the work functions were found to be 4.55 eV and 4.6 eV at 25 and 44 hours, respectively. Auger data indicated an increase in carbon content for both films. This may account for the slight appearance of two work functions on the Fowler plots of each film's last data set.

NbC/Nb Film #1

This particular film was loaded into the UHV chamber the same day it was deposited. Immediately after a suitable chamber vacuum (around 5×10^{-8} Torr) had been reached, the first set of photoemission data was taken. Extrapolated Fowler plots showed the work function at this time to be about 4.32 eV. Subsequent data taken 42 hours later still yielded a work function around 4.3 eV. The film was then sputtered in a static argon environment for 30 minutes. Upon completion of the sputtering, the work function was found to be 4.4 eV.

Auger scans were taken both before and after the film was sputtered. Before the sputtering, the niobium and carbon levels were around 25% and 44%, respectively. After the film was sputtered with argon, the niobium level rose to about 31%, while the carbon level fell to 37%. The oxygen level showed only a slight rise after the sputtering. It

appears that the argon sputtering succeeded in cleaning up the surface of the film. However, the sputtering away of surface carbon led to an increase in the film's work function.

NbC/Nb Film #2

This film was loaded into the UHV system about 67 days after it was deposited. The first set of photoemission data was taken 96 hours after the establishment of a 5×10^{-8} Torr vacuum. The work function at this time was found to be 4.3 eV. The film was then sputtered with oxygen for 15 minutes. What was the energy of the oxygen ions? Data taken 20 hours after sputtering showed that the work function had risen to 4.65 eV.

Auger scans taken before the oxygen sputtering showed niobium and carbon levels of 23% and 30%, respectively. After sputtering, the niobium level rose to around 30% while carbon fell to about 22%. Once again, the oxygen level on the surface of the film rose only slightly after sputtering. The auger and work function data taken 20 hours after sputtering yielded both the lowest level of carbon and the highest work function of any previous data taken on this material.

NiNb/Nb Film #1

This particular film was loaded into the UHV chamber 52 days after it was deposited. 24 hours after a vacuum of 2×10^{-8} Torr was established, an attempt was made to gather photoemission data. However, due to poor contact with the film surface, a usable set of data was not collected until 190 hours after a suitable vacuum was achieved. The first usable set of data revealed what appeared to be two separate work functions, one around 4.49 eV and another at about 4.3 eV. Auger data taken at this time showed oxygen around 57%, while carbon, nickel, and niobium were all found to be in the 12% to 15% range.

The next set of photoemission figures was taken 60 hours after the UHV chamber was baked at 200°C. Once again there appeared to be two separate work functions, one at 4.5 eV and another at 4.35 eV. The only significant surface chemistry changes observed after baking involved a near doubling of carbon from 15% to 29%, and a decrease in oxygen to around 46%.

The last few data sets were taken after the film was exposed to air for about 2.5 hours. The first photoemission readings taken 24 hours after the exposure of air yielded work function values of 4.4 eV and 4.6 eV. Auger scans showed oxygen with a slight increase to 52%, while carbon content decreased to 23%. With the exception of a slight increase in nickel content, work function and surface chemistry data at 7 days after air exposure did not signal any significant changes.

Pt Film #1

Pt Film #1 was loaded into the UHV chamber 2 days after it was deposited. Photoemission data were taken 1 hour after achieving a $5 \leftrightarrow 10^{-8}$ Torr vacuum. A Fowler plot of this data yielded a work function of about 4.82 eV. Auger scans of the film surface showed the average platinum level to be around 92%, while carbon averaged 7.5%. Oxygen comprised less than 1% of the film surface. Another set of photocurrent readings taken 120 hours after vacuum indicated that the work function had decreased to 4.7 eV. Meanwhile, Auger data showed a slight decrease in oxygen and about a 2.5% rise in the carbon level. The amount of platinum on the film surface appeared to decline about 2%.

PtC/Pt Film #1

Pt/C Film #1 was loaded into the UHV chamber 56 days after it was deposited. The first set of photoemission data was taken 24 hours after achieving a 2.2×10^{-8} Torr vacuum. A Fowler plot of this data revealed a work function around 4.57 eV. Auger analysis was not performed at this time. Another set of photocurrent readings were taken after the film had been in the UHV chamber for 190 hours. The work function had declined to around 4.22 eV. Auger scans showed the average surface composition of the film to be 74% platinum, 22% carbon, and 4% oxygen.

The UHV chamber was baked at 125°C for 12 hours. Photoemission data taken 60 hours later showed the work function to be 4.05 eV. Auger analysis revealed that the platinum level had declined to around 69%, while the average amount of surface carbon had increased to 26.5%. Meanwhile, the level of oxygen on the film surface did not significantly change.

The film was then exposed to air for 2.5 hours. After the exposure to air, the film was loaded back into the UHV chamber and a 1.0×10^{-8} Torr vacuum was established. A set of photocurrent readings taken 24 hours later yielded a work function around 4.43 eV. Auger data showed only a slight decline in the platinum level, while the amount of carbon on the film surface decreased to around 20%. At the same time, oxygen increased to an average level of 10%. When photoemission data were taken 21 days after air exposure, the work function stood at 4.4 eV. The level of surface platinum was around 72.5%, while carbon and oxygen content averaged 23% and 4.5%, respectively.

Ru/Ta Film #1

This film was loaded into the UHV chamber 1 day after its deposition. The first set of photocurrent readings were taken 1 hour after a vacuum in the 10^{-8} Torr range was achieved. The work function at this time was about 4.85 eV. Since the primary Auger peaks for carbon and ruthenium are so close together, numerical interpretations of the Auger scans had the possibility of being misleading. However, unlike carbon, ruthenium has another Auger peak that can be used to monitor its rise or decline in relative surface level. Therefore, each Auger scan was examined and judgments were made regarding any obvious changes in ruthenium and oxygen.

After the film had been in vacuum for 93 hours, data showed a lower work function of 4.4 eV. Auger scans taken at this time did not reveal any significant work function changes. Ta/Ru Film #2 was then removed from the system

and exposed to air for about 3 days. It was loaded back into UHV chamber and the chamber was then baked at 150°C for 10 hours. Subsequent photoemission data showed that the work function had decreased to 4.3 eV. Auger scans showed a possible increase in the level of ruthenium. However, due to a larger Auger peak where the primary ruthenium and carbon peaks are located, carbon level may have also increased. There appeared to be no change in the level of surface oxygen.

The UHV chamber was again baked at 150°C, this time for 12 hours instead of 10. Data taken 21 hours later showed a work function in the range of 4.0 eV - 4.1 eV. Auger scans did not appear to be much different from the scans taken after the first baking.

Ru/Ta Film #2

Ruthenium will not oxidize at atmospheric pressure until it reaches a temperature of about 800°C. Therefore, 13 days after deposition, Ta/Ru Film #3 was put into a quartz glass tube oven and baked to 800°C. While baking, a continuous stream of oxygen gas flowed through the tube.

Before loading the film into the UHV chamber, a resistance on the order of 10^9 Ω was found across the surface of the film. This was most likely due to the formation of tantalum oxide, an insulator, on the surface of the film. The high resistance was a concern because the film surface must be grounded when taking auger scans. However, because photocurrent readings on previous films of this material were found to be no greater than 10^{-11} A, the resistance was not expected to interfere with the gathering of photoemission data. The film was loaded into the UHV chamber about 1 day after baking in the tube oven.

The first set of photoemission data were taken 3 hours after a vacuum of 5×10^{-8} Torr was established. Work function appeared to be around 4.5 eV. Attempts to Auger the film were unsuccessful due to the high resistance discussed previously. The last set of photoemission data on this film was taken 21 hours after establishing a suitable vacuum. The work function at this time was found to be between 4.35 - 4.4 eV.

Ru/Ta Film #3

This particular film was loaded into the UHV chamber 1 day after it was deposited. Photoemission data taken after achieving a 5×10^{-8} Torr vacuum revealed a work function of 4.7 eV. After 16 hours, auger scans showed a decrease in surface oxygen levels and photoemission data indicated a work function around 4.42 eV.

At this point in the research, the UHV system appeared to have a leak. Upon further inspection, the problem was traced to a failure in some welds near the ion pump. The system was disassembled and the areas of leakage were re-welded. Ta/Ru Film #4 was exposed to air during the approximately 25 - 30 days that the vacuum system was down.

The next set of photoemission data were taken after the repaired vacuum system was brought to a pressure of 3×10^{-8} Torr. The work function appeared to be around 4.55 eV. Auger data showed an increase in surface oxygen, as well as a decrease in ruthenium levels. The UHV system was then baked at 150°C for 12 hours. Data taken 12 hours later showed a work function between 4.4 and 4.45 eV. Auger scans taken at this time indicated a decline in surface oxygen content.

ZrC/Mo Film #1

This film was loaded into the UHV chamber 2 days after it was deposited. A vacuum around 5×10^{-8} Torr was established and 120 hours later, the first set of photocurrent readings was taken. A work function between 4.35 and 4.5 eV was extrapolated from a Fowler plot that was mostly non-linear. An analysis of Auger scans taken at this time revealed a surface that was averaged about 87% carbon, 9% oxygen, and 4% zirconium.

The film was then sputtered with argon for about 30 minutes. Data taken immediately after the sputtering revealed that the work function had risen to about 4.75 eV. Meanwhile, Auger data showed that while the oxygen level decreased, surface carbon appeared to increase. Zirconium levels at this time remained constant.

ZrC/Mo Film #2

ZrC/Mo Film #2 was loaded into the UHV chamber 1 day after its deposition. Photoemission data taken 4 hours after achieving a 5×10^{-8} Torr vacuum revealed a work function around 4.2 eV. Auger scans taken at this time showed the oxygen level ranging from 53% to 67%, while zirconium content ranged from 16% to 31%. Meanwhile, surface carbon levels averaged around 16.5%.

The film was then sputtered with argon for 30 minutes. Data taken immediately after sputtering revealed a work function around 4.15 eV. Surface analysis showed the oxygen level ranging from 51% to 83.5%, while zirconium appeared to be as low as 4.5% and as high as 20%. Carbon content data also lacked consistency as it ranged from 12% to 29%.

ZrC/Mo Film #3

This film was loaded into the UHV chamber 3 days after its deposition. Photocurrent readings were taken 1 hour after a vacuum of 5×10^{-8} Torr was established. This data revealed a work function around 4.4 eV. Auger scans revealed a surface that averaged 65% oxygen, 28% zirconium, and 7% carbon. After 22 hours in the vacuum, the work function fell to 4.27 eV. While Auger scans taken at this time showed no significant change in zirconium, the carbon level increased, with surface percentages ranging from 15% to 35.5%. At the same time, the average oxygen level on the surface declined, with values that ranged from 41% to 61%.

The film was then sputtered with argon for 35 minutes. Photoemission data taken immediately after sputtering revealed a work function between 4.5 and 4.55 eV. Auger analysis performed after sputtering showed an increase in

oxygen and a decrease in surface carbon. Oxygen values now ranged from 59% to 71%, while carbon percentages varied from 10% to 16%. The zirconium level slightly declined, with an average surface percentage of 22%.

Ta Film #1

This film was loaded into the UHV chamber 1 day after its deposition. A vacuum of 5 $\leftrightarrow$ 10^{-8} Torr was established and, 1 hour later, the first set of photoemission data was taken. This data showed the work function to be around 4.1 eV. Auger scans indicated that the film surface was approximately 50% oxygen, 44.5% tantalum, and 5% carbon. After the film had been in a vacuum for 121 hours, another set of photocurrent readings were taken. The work function appeared to have dropped to 4.0 eV. Auger analysis yielded a film surface comprised, on average, of 48.5% oxygen, 41.5% tantalum, and 10% carbon.

Table 6. Work function of the films measured for the samples which were exposed only to air and for the samples exposed to 20 min. of ozone.

Material	No Exposure to O_3		20 min. Exposure to O_3	
	Work Function (eV)	Composition (%)	Work Function (eV)	Composition (%)
MgPt	4.1	0.48 Mg, 0.48 O, 0.03 Pt	4.38	0.09 Pt, 0.36 O, O.56 Mg
Mo	4.6			
Nb	4.25 4.3 4.55 4.6	0.15 C, 0.57 O 0.20 C, 0.63 O		
NbC/Nb	4.32 4.40 4.65	0.25 Nb, 0.44 C 0.31 Nb, 0.37 C 0.30 Nb, 0.22 C	4.41	0.19 Zr, 0.19 C, 0.61 O
NbNi/Nb	4.49, 4.3 4.35	0.57 O, 0.12-0.15 Nb,C,Ni 0.46 O, 0.29 C	4.51	0.15 Nb, 0.24 Ni, 0.12 C, 0.5 O
Pt	4.82	0.92 Pt, 0.07 C, <0.01 C	5.13	0.94 Pt, 0.06 C, 0.01 O
C/Pt	4.57 4.22 4.05 4.4	 0.74 Pt, 0.22 C, 0.04 O 0.69 Pt, 0.26 C 0.72 Pt, 0.23 C, 0.04 O	4.79	0.86 Pt, 0.02 C, 0.12 O
Ru/Ta	4.85, 4.4, 4.3, 4.0-4.1		4.78	
RuTa/Ta	4.42		4.41	
Ta	4.1 4.0	0.50 O, 0.44 Ta, 0.05 C 0.48 O, 0.42 Ta, 0.10 C	4.16	
ZrC/Mo	3.65-3.7, 3.9 4.35, 4.5 4.4	 0.87 C, 0.09 O, 0.04 Zr 0.07 C, 0.65 O, 0.28 Zr	4.91	0.22 Mo, 0.12 C, 0.66 O

CONCLUSIONS

Some of the results of this materials investigation are summarized in Table 7. They suggest that NbC/Nb, NbNi/Nb, and MgPt are the materials that are the most compatible with the electrodynamic tether application. However, the sputter yields of MgPt/Pt and NbNi/Nb must still be assessed to determine if they are compatible with the application, and the conductivity of NbC/Nb must be assessed to determine if the conductivity of the oxidized material is acceptable. The critical results that lead to the elimination of several candidates are summarized as:

ZrC/Mo: Work function increase from oxygen exposure was too high.

Ru/Ta: Work function increase from oxygen exposure was too high.

RuTa/Ta: Resistivity increase from oxygen exposure was too high.

C/Pt: Work function increase from oxygen exposure was too high.

MgPt: Work function and resistivity changes from oxygen exposure are acceptable.

There are other very insightful results of this investigation:

-The ZrC surface film oxidizes, but passivates in thickness-not in concentration, and protects the Mo base from oxidation.

-The Nb base film has an extremely high affinity for oxygen, therefore it is unintentionally deposited as an oxide with an acceptable work function, but unacceptable conductivity.

-Ta and Mo are also easily oxidized with no passivation and unacceptable conductivity.

This research should be continued with experimental and theoretical programs. Measurements should be conducted on oxide films including NiO/Nb, MgO/Pt, RuO_2/Ta and IrO_2/Ir for comparison. The effect of an oxide film on the tip conductivity and ultimately the work function should be modeled so that the tolerable characteristics of the oxide can be identified.

Sample Identity	Surface Film	Thickness (nm)	Base film	Thickness (nm)	Initial Φw (eV)	Final Φw (eV)	Initial R (mOhms)	Final R (mOhms)
Ideal						**<4.8**		**<74**
MgPt			MgPt	200	4.1	4.38	30	30
Mo			Mo	300	4.6		74	??
Nb			Nb	300	4.25-4.6		74	??
NbC/Nb	NbC	10	Nb	500	4.32-4.65	4.41	43	??
NbNi/Nb	NbNi	10	Nb	300	4.3-4.49	4.51	50	45
Pt			Pt	200	4.82	5.13	47	45
PtC/Pt	PtC	10	Pt	200	4.05-4.57	4.79	26	??
Ru/Ta	Ru	10	Ta	300	4.0-4.85	4.78	54	??
RuTa/Ta	RuTa	10	Ta	300		4.41	114	127
Ta			Ta	300	4.0-4.1	4.16	261	265
ZrC/Mo	ZrC	10	Mo	300	3.65-4.5	4.91	176	173

ACKNOWLEDGEMENTS

The authors would also like to gratefully acknowledge NASA MSFC (John Cole, Dr. Kai Hwang, Randy Bagget, Les Johnson) and Tethers Unlimited Inc. (Dr. Rob Hoyt) for funding the development of field emission cathodes for space-based applications and Drs. Capp Spindt, Babu Chalamala and Paul McClelland for their valuable advice on field emission cathode operation and materials. The research described in this paper was carried out at the Jet Propulsion Laboratory, California Institute of Technology, under a contract with the National Aeronautics and Space Administration

REFERENCES

Marrese, C. M., Wang, J., Goodfellow, K. D., Gallimore, A. D., "Space-Charge Limited Emission from Field Emission Array Cathodes for Electric Propulsion and Tether Applications," *Micropropulsion for Small Spacecraft*, AIAA Progress Series Vol. 187, edited by M. Micci and A. Ketsdever, AIAA , Reston, VA, 2000, Chapter 18.

Brodie, I. and Spindt, C. A. "Vacuum microelectronics," Adv. Electron. Electron Phys., vol.83, p.1, 1992.

Chalamala, B. R. , Wallace, R. M. , Gnade, B. E. , "Effect of O_2 on the electron emission characteristics of active molybdenum field emission cathode arrays," J. Vac. Sci. Technol. B 16(5), Sep/Oct 1998.

Marrese, C. M., Polk, J., Jensen, K., "Experimental Performance Evaluations of Mo and ZrC-Coated Mo Field Emission Array Cathodes in Oxygen Environments," IEPC Paper No. 01-278, , 27th International Electric Propulsion Conference, October 2001, Pasadena, CA.

Shaw, J. "Effects of surface oxides on field emission from silicon," J. Vac. Sci. Technol. B 18(4), Jul/Aug 2000.

Tsarev, B.M., *Contact Difference of Potentials*, State Techn. and Theoret. Press, Moscow (1955), p. 166.

Fomenko, V. S., *Handbook of Thermionic Properties:Electronic Work Functions and Richardson Constants of Elements and Compounds*, Plenum Press Data Division, New York, 1966.

Jentzsch, F., Ann. Phys. 27:129, 1908.

Spanner, H., Ann.Phys.27:609, 1924.

Mackie, W. A., Cabe, G. L., Southall, L.A., Xie, T., McClelland, P.H., "Materials Deposition and Emission Characteristics of NbC/Nb Field Emitter Array Cathode," IVMC, Aug 2001, Davis, CA.

Yoon, J. Y., Yoon, D., Baik, H. K., Lee, S., Song, K. M., Lee, S., "Suppression of oxidation of metal emitters by incorporating ruthenium oxide," J. Vac. Sci. Technol. B 18(2) Mar/Apr 2000.

Ziegler, J.F., Biersack, J.P., and Littmark, U., "The Stopping Range of Ions in Matter," Permagon Press, New York, 1985. (new edition in late 1996).

[1] http://www.SRIM.org/